SU(3) flavor symmetry analysis of hyperon non-leptonic two body decays*

Xin Wu (吴鑫)[1,2] Qi Chen (陈奇)[1,2] Ye Xing (邢晔)[3] Zhi-Peng Xing (邢志鹏)[1,2†] Ruilin Zhu (朱瑞林)[1,2‡]

[1]Department of Physics and Institute of Theoretical Physics, Nanjing Normal University, Nanjing 210023, China
[2]Nanjing Key Laboratory of Particle Physics and Astrophysics
[3]School of Physics,China University of Mining and Technology, Xuzhou 221000, China

Abstract: This paper presents a systematic study of hyperon non-leptonic two-body decays induced by light quark transitions, particularly the $s \to u\bar{u}d$ process, within the framework of $SU(3)$ flavor symmetry. The effective weak Hamiltonian is decomposed into irreducible $SU(3)$ representations, including the 27-plet and octet components, and applied to analyze decays of octet and decuplet baryons and charmed baryons. Both the irreducible representation amplitude (IRA) approach and the topological diagrammatic analysis (TDA) are employed to construct decay amplitudes and constrain the parameter space. $SU(3)$ symmetry-breaking effects arising from the strange quark mass are incorporated systematically. A global fit to current experimental data allows us to extract form factors and predict branching ratios and asymmetry parameters for several decay channels. Our results demonstrate the predictive power of $SU(3)$ flavor symmetry while highlighting significant symmetry-breaking effects, especially in amplitudes related to the 27-plet. Notably, the $\Sigma^+ \to p\pi^0$ decay channel exhibits a deviation exceeding 1σ from experimental measurements, suggesting the possible presence of new decay mechanisms or contributions beyond the Standard Model. Besides, we also evaluate the size of symmetry breaking. However, the large uncertainty of the experimental data makes it difficult to precisely determine the value of symmetry breaking. We strongly recommend that future experimental efforts aim to reduce the measurement uncertainties, especially for the processes $\Lambda^0 \to p\pi^-$ and $\Lambda^0 \to n\pi^0$, which have larger experimental errors compared to other data and play an important role in determining the symmetry breaking parameter. This study provides a systematic framework for future tests of the Standard Model and the search for new physics in hyperon decays.

Keywords: $SU(3)$ flavor symmetry, hyperon decays, weak decays

DOI: 10.1088/1674-1137/adf1f1 **CSTR:** 32044.14.ChinesePhysicsC.49123101

I. INTRODUCTION

Weak decays of hyperons have long constituted a crucial issue for testing the Standard Model (SM) and exploring new physics (NP). From the experimental side, hyperons, as intermediate states in heavy hadron cascade decay processes, are abundantly produced due to their low production threshold at many experimental facilities such as BESIII and LHCb [1−7]. Recently, BESIII has reported new measurements for the absolute branching fraction of $\Omega^- \to \Xi^0\pi^-$, $\Omega^- \to \Xi^-\pi^0$, $\Omega^- \to \Lambda^0 K^-$ decay, and the sensitivity is now in the range of $10^{-5} \sim 10^{-8}$ [8]. From the theoretical side, hyperon weak decays involve a large CKM matrix element $V_{us}V_{ud}^*$. The precise testing of this CKM matrix element is helpful for testing the unitarity of the CKM matrix. In addition, due to their low threshold, hyperons exhibit rich non-perturbative QCD effects and distinct decay behaviors, which are reflected in their complex angular distributions [9]. In recent years, there has been much theoretical work focusing on hyperon decays such as the structure of hyperons [10], decay mechanism [11], angular distribution [12].

As for the theoretical study of the hyperon decays, strict factorization does not work well due to the low threshold and the smaller transform energy in the s quark decay modes. Therefore, the perturbative calculation is currently not feasible. Besides the perturbative study, model calculation [11, 13−16], effective theory [17−21], symmetry analysis [22−24], Lattice QCD [25, 26], and related approaches [27−29] still work well in hyperon de-

Received 29 May 2025; Accepted 15 July 2025; Published online 16 July 2025

* Ruilin Zhu is supported by NSFC (12322503, 12075124) and the Natural Science Foundation of Jiangsu (BK20211267). Zhi-Peng Xing is supported by NSFC (12375088, 12335003, 12405113). Ye Xing is supported by NSFC (12005294)

† E-mail: zpxing@nnu.edu.cn
‡ E-mail: rlzhu@njnu.edu.cn

cays. However, due to their large model independence, the uncertainty in model calculation is difficult to estimate [11]. Effective theories such as Chiral perturbation theory (χPT) have been highly successful in studying low-energy strong interaction physics. However, they may require further investigation to address the puzzle of $\alpha(\Sigma^+ \to p\gamma)$ [19]. As a symmetry analysis method, although the $SU(3)$ analysis does not involve detailed dynamic understanding, it seems that it can solve this problem [30]. Therefore, the analysis of the hyperon decays in $SU(3)$ symmetry is useful.

In symmetry analysis, although it is not possible to calculate the absolute values of the decay amplitudes, it can be used to obtain relations between different decay amplitudes. With a smaller number of amplitudes, when combined with experimental data, the amplitudes can be constrained and predictions can be made to further test the approach without a detailed understanding of the dynamics. Recently, there have been many symmetry analysis works on the hyperon decay processes [22−24]. As an important part of hyperon decays, hyperon non-leptonic two body decays have accumulated a large amount of experimental data and rich phenomenological observables, which have attracted considerable interest from theorists. In these processes, symmetry analyses such as isospin symmetry, which reflects the up and down quark symmetry, have been previously studied [22]. Although the isospin symmetry is powerful in hyperon non-leptonic two body weak decay processes, the $SU(3)$ symmetry which reflects the u, d, s symmetry, requires fewer parameter and can provide more information, such as the CPV. We note that a preliminary $SU(3)$ topological diagram analysis has been presented [23]. Unfortunately, an $SU(3)$ symmetry analysis based on strict irreducibility representation decomposition is still absent in these processes. Therefore, further $SU(3)$ symmetry analysis of hyperon non-leptonic two body decay processes is both necessary and urgent.

The rest of this paper is organized as follows. In Sec. II, the theoretical framework of hyperon non-leptonic two body weak decay under $SU(3)$ symmetry is described. The decomposition of the Hamiltonian, which is the $3\otimes3\otimes\bar{3}\otimes\bar{3}$ $SU(3)$ group representation, is derived for the first time. In Sec. III, the octet light baryon two body decays are studied under $SU(3)$ symmetry. Subsequently, the decuplet light baryon two body decays are analyzed in Sec. IV. Induced by the same Hamiltonian, the charmed baryon and octet light meson decay can also be studied, which are presented in Sec. V and Sec. VI, respectively. The conclusions are presented in the last section.

II. THEORETICAL FRAMEWORK

Under $SU(3)$ symmetry, baryons composed of light quarks can be classified into an octet and a decuplet, while light mesons form an octet. To study the hyperon two body weak decays, the effective Hamiltonian is given as [31]

$$\mathcal{H}_{\rm eff} = \frac{G_F}{\sqrt{2}} V_{ud}V_{us}^* \sum_{i=1}^{10} \left[z_i(\mu) - \frac{V_{td}V_{ts}^*}{V_{ud}V_{us}^*} y_i(\mu) \right] Q_i(\mu), \quad (1)$$

where V_{uq} is the CKM matrix element and z_i and y_i are the Wilson coefficients. For the current-current operator $Q_{1/2}$, which is proportional to $V_{ud}V_{us}^*$, we have $y_{1/2} = 0$. For the penguin operator Q_{3-10}, which is proportional to $V_{td}V_{ts}^*$, we have $z_{3-10} = 0$. To study the primary contribution of the Hamiltonian, only the tree level operators Q_1 and Q_2 are considered in this study. These specific expressions of four-quark operator $Q_{1/2}$ are

$$\begin{aligned} Q_1 &= [\bar{d}_\alpha u_\beta]_{V-A}[\bar{u}_\beta s_\alpha]_{V-A}, \\ Q_2 &= [\bar{d}_\alpha u_\alpha]_{V-A}[\bar{u}_\beta s_\beta]_{V-A}. \end{aligned} \quad (2)$$

By extracting the flavor information, the tree level Hamiltonian can be redefined as

$$\mathcal{H}_{\rm eff} = \frac{G_F}{\sqrt{2}} V_{ud}V_{us}^* \times \sum_{\lambda=1,2} C_\lambda \sum_{i,j,k,l} (H_\lambda)^{ij}_{kl} \left[\bar{q}^i_\alpha q^k_\alpha\right]_{V-A} \left[\bar{q}^j_\beta q^l_\beta\right]_{V-A}, \quad (3)$$

where q^1, q^2, and q^3 correspond to the u, d, and s quark, respectively. The Wilson coefficient C_λ is $z_\lambda(\mu) - \frac{V_{td}V_{ts}^*}{V_{ud}V_{us}^*} y_\lambda(\mu)$. The matrix H_λ only contains two nonzero elements, $(H_2)^{21}_{13} = 1$ and $(H_1)^{12}_{13} = 1$, with $\lambda = 1, 2$.

In the $SU(3)$ irreducibility representation amplitude (IRA) method, the matrix H_λ can be seen as the $3\otimes3\otimes\bar{3}\otimes\bar{3}$ $SU(3)$ group representation, and it can be composed as $3\otimes3\otimes\bar{3}\otimes\bar{3} = 27\oplus10\oplus\overline{10}\oplus8\oplus8\oplus8\oplus8\oplus1\oplus1$. In preliminary analysis, it is known that the representations 27 and (10, $\overline{10}$) should be the symmetric traceless representations as $(H_{27})^{\{ij\}}_{\{kl\}}$, $(H_{10})^{\{ijm\}}$, and $(H_{\overline{10}})_{\{ijm\}}$. Both the traces in these representations are absorbed into the 8 and 1 representations. To construct these representation matrices, the Hamiltonian matrix H^{ij}_{kl} can be symmetrized and anti-symmetrized into four terms as follows

$$\begin{aligned} H^{ij}_{kl} &= H^{\{ij\}}_{\{kl\}} + H^{\{ij\}}_{[kl]} + H^{[ij]}_{\{kl\}} + H^{[ij]}_{[kl]}, \\ H^{\{ij\}}_{\{kl\}} &= \frac{1}{4}(H^{ij}_{kl} + H^{ji}_{kl} + H^{ij}_{lk} + H^{ji}_{lk}), \\ H^{\{ij\}}_{[kl]} &= \frac{1}{4}(H^{ij}_{kl} + H^{ji}_{kl} - H^{ij}_{lk} - H^{ji}_{lk}), \\ H^{[ij]}_{\{kl\}} &= \frac{1}{4}(H^{ij}_{kl} - H^{ji}_{kl} + H^{ij}_{lk} - H^{ji}_{lk}), \\ H^{[ij]}_{[kl]} &= \frac{1}{4}(H^{ij}_{kl} - H^{ji}_{kl} - H^{ij}_{lk} + H^{ji}_{lk}). \end{aligned} \quad (4)$$

$H^{\{ij\}}_{\{kl\}}$ contains the 27 representation and can be identified

directly. For constructing the 10 and $\overline{10}$ representation, the matrix can be defined as

$$H^{\{ij\}m} = \epsilon^{mkl} H^{\{ij\}}_{[kl]}, H_{\{kl\}n} = \epsilon_{ijn} H^{[ij]}_{\{kl\}}. \tag{5}$$

It is evident that only index ij are symmetric in $H^{\{ij\}m}$ and $k\ l$ are symmetric in $H_{\{kl\}n}$. After the symmetrized and anti-symmetrized processing, the complete symmetry matrix can be constructed as

$$\begin{aligned} H^{\{ij\}m} &= H^{\{i\{j\}m\}} + H^{\{i[j]m]} \\ &= \frac{3}{2} H^{\{ijm\}} - \frac{1}{2} H^{\{mj\}i} + \frac{1}{2}\epsilon^{jmn}\mathring{H}^i_n, \\ H_{\{kl\}n} &= H_{\{k\{l\}n\}} + H_{\{k[l]n]} \\ &= \frac{3}{2} H_{\{kln\}} - \frac{1}{2} H_{\{kl\}n} + + \frac{1}{2}\epsilon_{lnm}\dot{H}^m_k, \end{aligned} \tag{6}$$

with

$$\mathring{H}^i_n = \epsilon_{njm} H^{\{i[j]m]}, \ \dot{H}^m_k = \epsilon^{mln} H_{\{k[l]n]}. \tag{7}$$

Then, we can solve

$$\begin{aligned} H^{\{ijm\}} &= H^{\{ij\}m} - \frac{1}{9}\epsilon^{ijk}\mathring{H}^m_n - \frac{4}{9}\epsilon^{jmn}\mathring{H}^i_n + \frac{2}{9}\epsilon^{min}\mathring{H}^j_n, \\ H_{\{kln\}} &= H_{\{kl\}n} - \frac{1}{9}\epsilon_{klm}\dot{H}^m_n - \frac{4}{9}\epsilon_{lnm}\dot{H}^m_k + \frac{2}{9}\epsilon_{nkm}\dot{H}^m_l. \end{aligned} \tag{8}$$

For the last term in Eq. (4), we can extract the octet 8 and singlet 1 as

$$\begin{aligned} H^{[ij]}_{[kl]} &= \frac{1}{2}\epsilon^{ijm}\epsilon_{kln}\ddot{H}^n_m + \frac{1}{6}(\delta^i_k\delta^j_l - \delta^i_l\delta^j_k)\overline{H}, \\ \ddot{H}^n_m &= \frac{1}{2}\epsilon_{ijn}\epsilon^{klm} H^{[ij]}_{[kl]} - \frac{1}{3}\delta^m_n H^{[ij]}_{[ij]}, \ \overline{H} = H^{[ij]}_{[ij]}, \end{aligned} \tag{9}$$

where $\ddot{H}^n_m$ refers to the traceless octet, and its trace corresponds to a singlet. Following the same method, $H^{\{ij\}}_{\{kl\}}$ can be decomposed into the 27, 8, and 1 representations as

$$\begin{aligned} H^{\{ij\}}_{\{kl\}} &= \tilde{H}^{\{ij\}}_{\{kl\}} + \frac{1}{5}(\delta^i_k\hat{H}^j_l + \delta^j_k\hat{H}^i_l + \delta^i_l\hat{H}^j_k + \delta^j_l\hat{H}^i_k) \\ &\quad + \frac{1}{12}(\delta^i_k\delta^j_l + \delta^i_l\delta^j_k)H, \end{aligned} \tag{10}$$

where $\tilde{H}^{\{ij\}}_{\{kl\}}$ is traceless. The irreducibility representation can be redefined as

$$\begin{aligned} &\tilde{H}^{\{ij\}}_{\{kl\}} \to (H_{27})^{\{ij\}}_{\{kl\}}, \ H^{\{ijm\}} \to (H_{10})^{ijm}, \\ &H_{\{kln\}} \to (H_{\overline{10}})_{kln}, \ \hat{H}^m_n \to (H^1_8)^m_n, \ \mathring{H}^m_n \to (H^2_8)^m_n, \\ &\dot{H}^m_n \to (H^3_8)^M_n, \ \ddot{H}^m_n \to (H^4_8)^m_n, \ H \to H^1_1, \quad \overline{H} \to H^2_1. \end{aligned} \tag{11}$$

Finally, the Hamiltonian matrix H^{ij}_{kl} can be decomposed by irreducibility representations as

$$\begin{aligned} H^{ij}_{kl} &= (H_{27})^{\{ij\}}_{\{kl\}} + \frac{1}{2}\epsilon_{klm}(H_{10})^{ijm} + \frac{1}{2}\epsilon^{ijn}(H_{\overline{10}})_{kln} \\ &\quad + \frac{1}{5}A^{ijn}_{klm}(H^1_8)^m_n - \frac{1}{6}B^{ijn}_{klm}(H^2_8)^m_n - \frac{1}{6}C^{ijn}_{klm}(H^3_8)^m_n \\ &\quad + \frac{1}{2}\epsilon^{ijn}\epsilon_{klm}(H^4_8)^m_n + \frac{1}{12}(\delta^i_k\delta^j_l + \delta^i_l\delta^j_k)H^1_1 \\ &\quad - \frac{1}{6}(\delta^i_k\delta^j_l - \delta^i_l\delta^j_k)H^2_1, \end{aligned} \tag{12}$$

with

$$\begin{aligned} A^{ijn}_{klm} &= \delta^i_k\delta^j_m\delta^n_l + \delta^j_k\delta^i_m\delta^n_l + \delta^i_l\delta^j_m\delta^n_k + \delta^j_l\delta^i_m\delta^n_k, \\ B^{ijn}_{klm} &= \delta^i_k\delta^j_m\delta^n_l + \delta^j_k\delta^i_m\delta^n_l - \delta^i_l\delta^j_m\delta^n_k - \delta^j_l\delta^i_m\delta^n_k, \\ C^{ijn}_{klm} &= \delta^i_k\delta^j_m\delta^n_l - \delta^j_k\delta^i_m\delta^n_l + \delta^i_l\delta^j_m\delta^n_k - \delta^j_l\delta^i_m\delta^n_k. \end{aligned} \tag{13}$$

Then, these irreducibility representations can be extracted as

$$\begin{aligned} (H_{27})^{\{ij\}}_{\{kl\}} &= H^{\{ij\}}_{\{kl\}} - \frac{1}{5}A^{ijn}_{klm}(H^1_8)^m_n - \frac{1}{12}(\delta^i_k\delta^j_l + \delta^i_l\delta^j_k)H^1_1, \\ (H_{10})^{ijm} &= H^{ij}_{kl}\epsilon^{m)kl}, \ (H_{\overline{10}})_{kln} = \epsilon_{ij\{n}H^{ij}_{kl\}}, \\ (H^1_8)^m_n &= H^{\{im\}}_{\{in\}} - \frac{1}{3}\delta^m_n H^{\{ij\}}_{\{ij\}}, \\ (H^2_8)^m_n &= H^{\{mj\}}_{nj\}} - H^{jm}_{\{nj\}}, \ (H^3_8)^m_n = H^{mj}_{\{nj\}} - H^{jm}_{\{nj\}}, \\ (H^4_8)^m_n &= \frac{1}{2}\epsilon_{ijn}\epsilon^{klm}H^{[ij]}_{[kl]} - \frac{1}{3}\delta^m_n H^{[ij]}_{[ij]}, \\ H^1_1 &= H^{\{ij\}}_{\{ij\}}, \ H^2_1 = H^{[ij]}_{[ij]}. \end{aligned} \tag{14}$$

A similar decomposition of the Hamiltonian is also employed in the analysis of tetraquarks in heavy meson weak decays [32]. After the decomposition, the specific expression of each irreducibility representation can be derived using the input Hamiltonian matrix. As the singlet is trivial, we have omitted it in the following analysis. However, it is noted that information from the Hamiltonian may provide further constraints on specific irreducibility representations. In the first step, the Hamiltonian in Eq. (3) can be redfined as $H_+ = (H_1 + H_2)/2$ and $H_- = (H_1 - H_2)/2$. The Hamiltonian can be expressed as

$$\begin{aligned} \mathcal{H}_{\rm eff} &= \frac{G_F}{\sqrt{2}} V_{ud}V^*_{us} \\ &\quad \times \sum_{\lambda=+,-} C_\lambda \sum_{i,j,k,l} (H_\lambda)^{ij}_{kl}[\bar{q}^i_\alpha q^k_\alpha]_{V-A}[\bar{q}^j_\beta q^l_\beta]_{V-A}, \end{aligned} \tag{15}$$

where $C_\pm = C_1 \pm C_2$. The index in H_+ is symmetric and H_- is anti-symmetric. This indicates that H_+ contains the H_{27}, H_{10}, $H_{\overline{10}}$, and $H^{1,2,3}_8$ irreducibility representations.

The matrix H_- only contains the H_8^4 representation. The Hamiltonian in Eq. (3) shows that the symmetry of the upper indices in H_λ is related to the lower indices. It can be expressed as

$$[\bar{q}^i_\alpha q^k_\alpha]_{V-A}[\bar{q}^j_\beta q^l_\beta]_{V-A} = [\bar{q}^j_\beta q^l_\beta]_{V-A}[\bar{q}^i_\alpha q^k_\alpha]_{V-A}. \tag{16}$$

This suggests that $(H_\lambda)^{ij}_{kl} = (H_\lambda)^{ji}_{lk}$. Then, we have

$$\begin{aligned} H^{\{ij\}}_{[kl]} &= \frac{1}{4}(H^{ij}_{kl} + H^{ji}_{kl} - H^{ij}_{lk} - H^{ji}_{lk}) = 0, \\ H^{[ij]}_{\{kl\}} &= \frac{1}{4}(H^{ij}_{kl} - H^{ji}_{kl} + H^{ij}_{lk} - H^{ji}_{lk}) = 0. \end{aligned} \tag{17}$$

Therefore, H_{10}, $H_{\overline{10}}$, H_8^2, and H_8^3 are equal to zero in this study.

III. OCTET LIGHT BARYON TWO BODY DECAYS

Using the Hamiltonian decomposition, the octet baryon two body decays $T_8 \to T_8 P_8$ are analyzed with the IRA method. The T_8 and P_8 respectively represent the light baryon octet and the pseudoscalar meson octet. They can be written as:

$$T_8 = \begin{pmatrix} \frac{\Sigma^0}{\sqrt{2}} + \frac{\Lambda}{\sqrt{6}} & \Sigma^+ & p \\ \Sigma^- & -\frac{\Sigma^0}{\sqrt{2}} + \frac{\Lambda}{\sqrt{6}} & n \\ \Xi^- & \Xi^0 & -\frac{2\Lambda}{\sqrt{6}} \end{pmatrix},$$

$$P = \begin{pmatrix} \frac{\pi^0 + \eta_q}{\sqrt{2}} & \pi^+ & K^+ \\ \pi^- & \frac{-\pi^0 + \eta_q}{\sqrt{2}} & K^0 \\ K^- & \bar{K}^0 & \eta_s \end{pmatrix}. \tag{18}$$

Following the analysis in Sec. II, the tree operators in Eq. (2) can be decomposed under the $SU(3)$ flavor symmetry as $3\otimes 3\otimes\bar{3}\otimes\bar{3} = 27\oplus 10\oplus\overline{10}\oplus 8\oplus 8\oplus 8\oplus 8\oplus 1\oplus 1$ and only 27 and 8 have nonzero contributions.

For the specific processes induced by $s \to u\bar{u}d$, the Hamiltonian matrices are $(H_+)^{12}_{13} = (H_+)^{21}_{13} = \frac{1}{2}$ and $(H_-)^{12}_{13} = -(H_-)^{21}_{13} = \frac{1}{2}$. The representations of the IRA Hamiltonian are

$$\begin{aligned} H^{\{12\}}_{27\{13\}} &= H^{\{21\}}_{27\{31\}} = H^{\{12\}}_{27\{31\}} = H^{\{21\}}_{27\{13\}} = \frac{1}{5}\sin\theta, \\ H^{\{22\}}_{27\{23\}} &= H^{\{22\}}_{27\{32\}} = H^{\{23\}}_{27\{33\}} = H^{\{32\}}_{27\{33\}} = -\frac{1}{10}\sin\theta, \\ H_{8\bar{3}}^2 &= \frac{1}{4}\sin\theta. \end{aligned} \tag{19}$$

Here, we define $|V_{ud}V^*_{us}| \sim \lambda \sim \sin\theta$, which reflects the CKM factor involved in the dominant tree-level weak transition $s \to u\bar{u}d$. This common factor is factored out from all decay amplitudes to simplify the $SU(3)$ analysis. As H_8^1 and H_8^2 have the same contribution for the $s \to u\bar{u}d$ transition, we only use H^8 to express these two octets. With the above expressions, one may derive the effective Hamiltonian for decays involving the octet baryon as

$$\begin{aligned} \mathcal{M}_{T_8\to T_8P_8} = {} & a_{27}(T_8)^j_i(H_{27})^{\{il\}}_{\{jk\}}(T_8)^m_l P_m \\ & + b_{27}(T_8)^j_i(H_{27})^{\{im\}}_{\{jk\}}(T_8)^k_l P^l_m \\ & + c_{27}(T_8)^j_i(H_{27})^{\{lm\}}_{\{jk\}}(T_8)^i_l P^k_m \\ & + d_{27}(T_8)^j_i(H_{27})^{\{lm\}}_{\{jk\}}(T_8)^k_l P^i_m \\ & + e_{27}(T_8)^l_i(H_{27})^{\{im\}}_{\{jk\}}(T_8)^j_l P^k_m \\ & + f_{27}(T_8)^m_i(H_{27})^{\{il\}}_{\{jk\}}(T_8)^j_l P^k_m \\ & + a_8(T_8)^j_i(H_8)^k_j(T_8)^l_k P^i_l \\ & + b_8(T_8)^j_i(H_8)^l_j(T_8)^i_k P^k_l \\ & + c_8(T_8)^k_i(H_8)^l_j(T_8)^j_k P^i_l \\ & + d_8(T_8)^l_i(H_8)^i_j(T_8)^j_k P^k_l \\ & + e_8(T_8)^l_i(H_8)^k_j(T_8)^j_k P^i_l, \end{aligned} \tag{20}$$

where $a_{27} \sim f_{27}$ and $a_8 \sim e_8$ are $SU(3)$ irreducible amplitudes. The expression shows that the amplitude of octet baryon two body decays $T_8 \to T_8P_8$ can be expressed by these 11 parameters. To determine these parameters, we used the experimental data presented in Table 2. Unfortunately, the current data are insufficient to determine these parameters. As each $SU(3)$ irreducible amplitude can be divided into parity conserving and parity violating terms, the total number of the IRA method parameters is 22, which is larger than the number of observables. Therefore, in this study, the number of $SU(3)$ irreducible amplitude is not counted correctly.

By including the color information in the Hamiltonian matrix, one finds that the two quark fields or anti-quark fields in $H^{\{ij\}}_{\{kl\}}$ are color symmetric and in $H^{[ij]}_{[kl]}$ are anti-symmetric. As the color must be anti-symmetric in the baryon state, the amplitude in which the initial/final baryon state directly connects to the two quarks/anti-quarks in the Hamiltonian is expected to be strongly suppressed [33, 34]. To correctly count the number of $SU(3)$ irreducible amplitudes, we can use the topological diagrammatic approach (TDA) method to provide an intuitive physical image. We find that for the color symmetric IRA Hamiltonian, only two topological diagrams (Fig. 1) can contribute. Then, the number of amplitudes of H_{27} and H_8^1 can be largely reduced. As the equivalence between the TDA and irreducible $SU(3)$ methods has been verified [35, 36], we convert the amplitude obtained

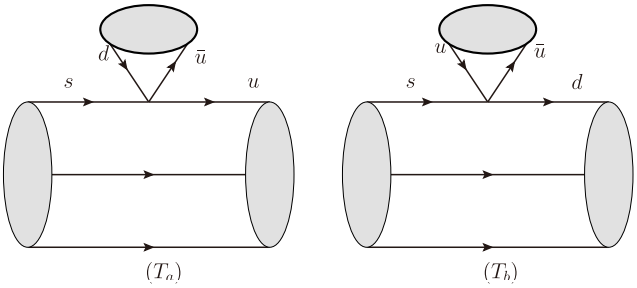

Fig. 1. Color symmetric topological diagrams for $T_8 \to T_8P_8$ nonleptonic decays.

using the TDA amplitude into IRA and only write down the IRA amplitude, which includes the contributions of the two topological diagrams in Fig. 1. We find that only two amplitudes c_{27} and e_{27} correspond to these two topological diagrams. The explicit expressions of these amplitudes are given as follows:

$$\begin{aligned}
T_a: (T_8)^{[in]j}H^{kl}_{mn}(T_8)_{[ik]j}P^m_l &= -(T_8)^l_i(H_{27})^{\{im\}}_{\{jk\}}(T_8)^j_l P^k_m \\
(T_8)^{[in]j}H^{kl}_{mn}(T_8)_{[kj]i}P^m_l &= (T_8)^j_i(H_{27})^{\{lm\}}_{\{jk\}}(T_8)^i_l P^k_m \\
&\quad + (T_8)^l_i(H_{27})^{\{im\}}_{\{jk\}}(T_8)^j_l P^k_m \\
T_b: (T_8)^{[in]j}H^{kl}_{mn}(T_8)_{[il]j}P^m_k &= -(T_8)^l_i(H_{27})^{\{im\}}_{\{jk\}}(T_8)^j_l P^k_m \\
(T_8)^{[in]j}H^{kl}_{mn}(T_8)_{[ij]l}P^m_k &= (T_8)^j_i(H_{27})^{\{lm\}}_{\{jk\}}(T_8)^i_l P^k_m \\
&\quad + (T_8)^l_i(H_{27})^{\{im\}}_{\{jk\}}(T_8)^j_l P^k_m. \qquad (21)
\end{aligned}$$

We find that the contribution of e_{27} in the two amplitudes contained in the topology $T_a(T_b)$ is opposite. As a result, they cancel each other when the amplitudes are summed, leaving only the contribution of c_{27}. Based on this simplification, the IRA amplitudes can be written as:

$$\begin{aligned}
\mathcal{M}_{T_8\to T_8P_8} &= c_{27}(T_8)^j_i(H_{27})^{\{lm\}}_{\{jk\}}(T_8)^i_l P^k_m \\
&\quad + a_8(T_8)^j_i(H_8)^k_j(T_8)^l_k P^i_l \\
&\quad + b_8(T_8)^j_i(H_8)^l_j(T_8)^i_k P^k_l \\
&\quad + c_8(T_8)^k_i(H_8)^l_j(T_8)^j_k P^i_l \\
&\quad + d_8(T_8)^l_i(H_8)^i_j(T_8)^j_k P^k_l \\
&\quad + e_8(T_8)^l_i(H_8)^k_j(T_8)^j_k P^i_l. \qquad (22)
\end{aligned}$$

Although the amplitude of H^1_8 can be largely reduced, the H^4_8, which comes from the $H^{[ij]}_{[kl]}$, will not be constrained. Therefore, the number of H_8 amplitudes remains 5. Form these amplitudes, we can derive the relations of the amplitudes by expanding them according to each decay channel in Table 2 as

$$\mathcal{M}(\Sigma^0 \to p\pi^-) = -\mathcal{M}(\Sigma^+ \to p\pi^0). \qquad (23)$$

In Eq. (22), there are 6 such amplitudes. In fact, these amplitudes can be expressed by 12 form factors. Generically, we can express them by parity conserving and parity violating as

$$\begin{aligned}
q_{27} &= G_F\bar{u}(f^c_{27} - g^c_{27}\gamma_5)u, \\
q_8 &= G_F\bar{u}(f^q_8 - g^q_8\gamma_5)u, \quad q = a,b,c,d,e. \qquad (24)
\end{aligned}$$

For the process of octet baryon two body decays $T_8 \to T_8P_8$, the non-polarization decay width is easily written as

$$\frac{d\Gamma}{d\cos\theta_M} = \frac{G_F^2|\vec{p}_{B_n}|(E_{B_n}+M_{B_n})}{8\pi M_{B_s}}(|F|^2+\kappa^2|G|^2), \qquad (25)$$

where $\hat{p}_{B_n}$ is final state momentum. Depending on the specific processes, the F and G linear functions of $f^i_{8/27}$ and $g^i_{8/27}$ are the scalar and peseudoscalar form factors, respectively. The parameter κ writing in terms of masses is given by

$$\kappa = |\vec{p}_{B_n}|/(E_{B_n}+M_{B_n}), \kappa^2 = \frac{(M_{B_s}-M_{B_n})^2-M_M^2}{(M_{B_s}+M_{B_n})^2-M_M^2}. \qquad (26)$$

Here M_{B_s}, M_{B_n}, and M_M are the masses of the initial octet baryons, final octet baryons, and mesons, respectively.

In this step, we find that the six $SU(3)$ parameters cannot explain the experimental data well. However, these results are not unexpected. The hyperon decays usually involve large $SU(3)$ symmetry breaking, considering the mass of strange quark. Therefore, in our analysis, the symmetry breaking should be considered.

As the mass of strange quark is much larger than that of the up and down quark, *i.e.*, $m_s \gg m_{u,d}$, the $SU(3)$ symmetry breakdown induced by the different masses of the light u, d, and s quarks can be introduced. The quark mass matrix can be written as

$$\begin{aligned}
M &= \begin{pmatrix} m_u & 0 & 0 \\ 0 & m_d & 0 \\ 0 & 0 & m_s \end{pmatrix} \sim m_u \begin{pmatrix} 1 & 0 & 0 \\ 0 & 1 & 0 \\ 0 & 0 & 1 \end{pmatrix} \\
&\quad + m_s \begin{pmatrix} 0 & 0 & 0 \\ 0 & 0 & 0 \\ 0 & 0 & 1 \end{pmatrix} = m_u \begin{pmatrix} 1 & 0 & 0 \\ 0 & 1 & 0 \\ 0 & 0 & 1 \end{pmatrix} + m_s \times \omega. \qquad (27)
\end{aligned}$$

The first matrix represents the mass term under the strict $SU(3)$ symmetry and the second matrix can be seen as an interaction term, which represents the $SU(3)$ symmetry breaking effect. Based on this mass matrix, the $SU(3)$ symmetry-breaking contributions to the irredu-

cible representation amplitudes can be constructed using the interaction matrix ω as:

$$\begin{aligned}\mathcal{M}^{SB}_{T_8\to T_8P_8} &= \mathbf{c^1_{27}}(T_8)^n_i(H_{27})^{lm}_{jk}(T_8)^i_lP^k_m\omega^j_n\\ &+\mathbf{c^2_{27}}(T_8)^j_i(H_{27})^{lm}_{jk}(T_8)^n_lP^k_m\omega^i_n\\ &+\mathbf{a_8}(T_8)^n_i(H_8)^k_j(T_8)^l_kP^i_l\omega^j_m\\ &+\mathbf{b^1_8}(T_8)^j_i(H_8)^l_j(T_8)^m_kP^k_l\omega^i_m\\ &+\mathbf{b^2_8}(T_8)^m_i(H_8)^l_j(T_8)^i_kP^k_l\omega^j_m\\ &+\mathbf{c^1_8}(T_8)^m_i(H_8)^l_j(T_8)^j_kP^i_l\omega^k_m\\ &+\mathbf{c^2_8}(T_8)^k_i(H_8)^l_j(T_8)^m_kP^i_l\omega^j_m\\ &+\mathbf{d_8}(T_8)^l_i(H_8)^i_j(T_8)^m_kP^k_l\omega^j_m\\ &+\mathbf{e_8}(T_8)^l_i(H_8)^k_j(T_8)^m_kP^i_l\omega^j_m. \end{aligned}\tag{28}$$

Although 9 SU (3) symmetry breaking terms were established, we found that the degrees of freedom of our IRA amplitude are only 7.

As the decay information expressed in the $SU(3)$ symmetry breaking terms $\mathbf{c^1_{27/8}}$, $\mathbf{a_8}$, $\mathbf{d_8}$, $\mathbf{e_8}$, and $\mathbf{b^1_8}$ is the same as that expressed in the corresponding $SU(3)$ symmetry terms, we can absorb these symmetry breaking contributions into the amplitude in Eq. (22). Finally, we found that only three $SU(3)$ symmetry-breaking terms remain.

$$\begin{aligned}\mathcal{M}^{SB}_{T_8\to T_8P_8} &= \mathbf{c^2_{27}}(T_8)^j_i(H_{27})^{lm}_{jk}(T_8)^n_lP^k_m\omega^i_n\\ &+\mathbf{b^2_8}(T_8)^j_i(H_8)^l_j(T_8)^m_kP^k_l\omega^i_m\\ &+\mathbf{c^2_8}(T_8)^m_i(H_8)^l_j(T_8)^j_kP^i_l\omega^k_m. \end{aligned}\tag{29}$$

Then, one can define new parameters A_8, B_8 to absorb the symmetry breaking terms $\mathbf{b^2_8}$ and $\mathbf{c^2_8}$ as $A_8 = a_8 - \mathbf{b^2_8} - 2\mathbf{c^2_8}$, $B_8 = b_8 + \mathbf{b^2_8}$. After the redefinition, the degrees of freedom are 8. Then, the amplitude $\mathbf{c_{27}}$ contains only the symmetry breaking contributions, while the other amplitudes are contributed by both symmetry and symmetry breaking terms. Therefore, the value of $\mathbf{c_{27}}$ represents the contribution of the symmetry breaking effect.

By the least-χ^2 fit method[37], we can perform a global analysis of these processes.

In this study, we find that the $SU(3)$ IRA amplitude, including symmetry breaking, can basically explain the experimental data, except the $Br(\Sigma^+\to p\pi^0)$ and $\alpha(\Sigma^+\to p\pi^0)$, which show more than 1σ deviation. By expanding the error of these two data points to 2σ, we can achieve a reasonable χ^2/d.o.f = 1.54.

The fitting parameters and prediction results are presented in Table 1 and Table 2. For the fitted parameters in , as the available experimental data are very limited, the constraints on each fitting parameter are rather weak, and the uncertainties for parameters with comparable contributions are generally similar. However, for c_{27} and $\mathbf{c^2_{27}}$, their contributions are relatively small, so they are less constrained by the experimental data, which leads to larger uncertainties. In particular, the contribution of c_{27} is smaller than that of $\mathbf{c^2_{27}}$, resulting in an even larger uncertainty for c_{27}. For the pseudoscalar form factors $g_{c_{27}}$, we notice this uncertainty is much larger. Although both scalar and pseudoscalar form factors contribute to the branching ratios (Br) and polarization parameter (α), the branching ratios are mainly determined by the scalar form factors. As a result, the pseudoscalar form factors are constrained almost exclusively by α, which also explains their relatively larger uncertainties.

Table 1. $SU(3)$ symmetry breaking irreducible amplitudes from fitting.

parameters	Our work	
	scalar(f)	pseudoscalar(g)
A_8	-3.20 ± 0.45	-1.74 ± 0.46
B_8	-3.32 ± 0.45	-10.49 ± 0.45
c_8	-2.39 ± 0.45	-8.84 ± 0.45
d_8	-3.04 ± 0.45	-2.64 ± 0.45
e_8	2.42 ± 0.45	2.48 ± 0.45
c_{27}	0.0672 ± 0.0010	0.031 ± 0.088
$\mathbf{c^2_{27}}$	-0.0503 ± 0.0032	-0.23 ± 0.12
χ^2/d.o.f	1.54	

Our results show that the puzzle of $\mathrm{Br}(\Sigma^+\to p\pi^0)$ and $\alpha(\Sigma^+\to p\pi^0)$ cannot be explained by the $SU(3)$ symmetry breaking effect. This suggests that the channel may involve a new decay mechanism, including possible contributions from new physics. We also look forward to future experiments, such as the Super Tau-Charm Facility (STCF), which can collect more data to reduce experimental errors and help resolve this puzzle. We also suggest that theorist pay more attention to this process.

To clearly see the contribution of H_8 and H_{27}, and the symmetry breaking term, we can factor out the corresponding wilson coefficient as [31]

$$C_+(1\ \mathrm{GeV}) = 0.680, \quad C_-(1\ \mathrm{GeV}) = -2.164. \tag{30}$$

The factored form factor can be defined as

$$\begin{aligned} &c^f_{27} = \frac{c_{27}}{C_+}, \qquad \mathbf{c^f_{27}} = \frac{\mathbf{c^2_{27}}}{C_+}, \qquad A^f_8 = \frac{A_8}{C_-},\\ &B^f_8 = \frac{B_8}{C_-}, \qquad q^f_8 = \frac{q_8}{C_-},\ q = c,d,e. \end{aligned}\tag{31}$$

Then, one can see that the factored out $SU(3)$ amplitudes c_{27}/C_+ and $\mathbf{c^2_{27}}/C_+$ are smaller than the amplitude

Table 2. Irreducible representation amplitudes (second column), experimental data (third column) and predicted values (fourth column) of the decay branching ratios, and experimental values (fifth column) and predicted values (sixth column) of the asymmetric parameters for the hyperon two-body non-leptonic decay.

Channel	Amplitudes	Br(10^{-2})		α	
		Experiment data	Our work	Experiment data	Our work
$\Sigma^0 \to p\pi^-$	$\frac{\sin\theta(5c_8-5d_8)}{20\sqrt{2}}$	–	$4.713(22)\times10^{-8}$	–	−0.99917(20)
$\Sigma^0 \to n\pi^0$	$\frac{\sin\theta(5c_8+5d_8+10e_8)}{40}$	–	$2.340(12)\times10^{-8}$	–	0.99620(47)
$\Lambda^0 \to p\pi^-$	$\frac{\sin\theta\left(-10b_8+5c_8-8c_{27}+5d_8-10\mathbf{b_8^2}-8\mathbf{c_{27}^2}\right)}{20\sqrt{6}}$	64.1(5)	64.1(5)	0.747(9)	0.747(9)
$\Lambda^0 \to n\pi^0$	$\frac{\sin\theta\left(10b_8-5c_8-12c_{27}-5d_8+10\mathbf{b_8^2}-12\mathbf{c_{27}^2}\right)}{40\sqrt{3}}$	35.9(5)	35.9(5)	0.692(17)	0.692(17)
$\Sigma^+ \to p\pi^0$	$\frac{\sin\theta(-5c_8+5d_8)}{20\sqrt{2}}$	51.47(30)	50.90(24)	−0.982(14)	−0.99904(22)
$\Sigma^+ \to n\pi^+$	$\frac{\sin\theta(5d_8+5e_8)}{20}$	48.43(30)	48.50(29)	0.0489(26)	0.0486(26)
$\Sigma^- \to n\pi^-$	$\frac{\sin\theta(5c_8+5e_8)}{20}$	99.848(50)	99.849(50)	−0.0680(80)	−0.0706(76)
$\Xi^- \to \Lambda^0\pi^-$	$\frac{\sin\theta\left(5a_8+5b_8-10c_8+4c_{27}-10\mathbf{c_8^2}\right)}{20\sqrt{6}}$	99.887(35)	99.887(35)	−0.390(7)	−0.390(7)
$\Xi^0 \to \Lambda^0\pi^0$	$\frac{\sin\theta\left(-5a_8-5b_8+10c_8+6c_{27}+10\mathbf{c_8^2}\right)}{40\sqrt{3}}$	99.524(12)	99.524(12)	−0.349(9)	−0.3490(89)

corresponding to H_8.

However, because all amplitudes corresponding to H_8 contain both symmetric and symmetry-breaking contributions, it is difficult to isolate the effects of *SU*(3) symmetry breaking in these channels. Fortunately, the amplitude $\mathbf{c_{27}}$ only contains the symmetry breaking contribution. Therefore, the ratio of form factor $R_f = \mathbf{f^c}_{27}/f^c_{27}$ and $R_g = \mathbf{g^c}_{27}/g^c_{27}$ can reflect the size of symmetry breaking as $R_f = -(75 \pm 5)\%$ and $R_g = -(742 \pm 2141)\%$. We can conclude that the symmetry breaking effect in the amplitude corresponding to H_{27} is at least 75%. However, we should also note that the form factor *g* indicated that these processes may contain a large symmetry breaking effect of up to $\sim 1000\%$. We strongly recommend that future experimental efforts aim to reduce the measurement uncertainties, especially the processes $\Lambda^0 \to p\pi^-$ and $\Lambda^0 \to n\pi^0$, which have larger experimental error compared to other data and play an important role in determining the parameter $\mathbf{c_{27}^2}$. Then, the extent of *SU*(3) symmetry breaking can be determined with higher precision.

IV. OTHER HYPERON TWO-BODY DECAYS INDUCED BY $s \to d$

Building upon the previous analysis of non-leptonic two-body decays of octet baryons, this section further extends the study to two-body decays of decuplet baryons and charmed baryons, which are induced by $s \to d$. Although these processes involve different types of particles, the Hamiltonian can also be treated with the same method. By decomposing the effective weak Hamiltonian into irreducible representations of *SU*(3), we can systematically construct the amplitude structures for various decay processes.

A. Decuplet baryon two body decays

The light baryons decuplet T_{10} can be written as a flavor matrix as

$$
\begin{aligned}
&T_{10}^{111} = \Delta^{++}, T_{10}^{112} = \frac{\Delta^+}{\sqrt{3}}, T_{10}^{113} = \frac{\Sigma^{*+}}{\sqrt{3}},\\
&T_{10}^{121} = \frac{\Delta^+}{\sqrt{3}}, T_{10}^{122} = \frac{\Delta^0}{\sqrt{3}}, T_{10}^{123} = \frac{\Sigma^{*0}}{\sqrt{6}},\\
&T_{10}^{131} = \frac{\Sigma^{*+}}{\sqrt{3}}, T_{10}^{132} = \frac{\Sigma^{*0}}{\sqrt{6}}, T_{10}^{133} = \frac{\Xi^{*0}}{\sqrt{3}},\\
&T_{10}^{211} = \frac{\Delta^+}{\sqrt{3}}, T_{10}^{212} = \frac{\Delta^0}{\sqrt{3}}, T_{10}^{213} = \frac{\Sigma^{*0}}{\sqrt{6}},\\
&T_{10}^{221} = \frac{\Delta^0}{\sqrt{3}}, T_{10}^{222} = \Delta^-, T_{10}^{223} = \frac{\Sigma^{*-}}{\sqrt{3}},\\
&T_{10}^{231} = \frac{\Sigma^{*0}}{\sqrt{6}}, T_{10}^{232} = \frac{\Sigma^{*-}}{\sqrt{3}}, T_{10}^{233} = \frac{\Xi^{*-}}{\sqrt{3}},\\
&T_{10}^{311} = \frac{\Sigma^{*+}}{\sqrt{3}}, T_{10}^{312} = \frac{\Sigma^{*0}}{\sqrt{6}}, T_{10}^{313} = \frac{\Xi^{*0}}{\sqrt{3}},\\
&T_{10}^{321} = \frac{\Sigma^{*0}}{\sqrt{6}}, T_{10}^{322} = \frac{\Sigma^{*-}}{\sqrt{3}}, T_{10}^{323} = \frac{\Xi^{*-}}{\sqrt{3}},\\
&T_{10}^{331} = \frac{\Xi^{*0}}{\sqrt{3}}, T_{10}^{332} = \frac{\Xi^{*-}}{\sqrt{3}}, T_{10}^{333} = \Omega^-.
\end{aligned}
\tag{32}
$$

Using the decomposed Hamiltonian in Eq. (18), we can construct the decuplet baryon two body decays as

$$\begin{aligned}\mathcal{M}_{10\to 8+8} = {} & a_{27}(T_{10})^{ijk}(H_{27})^{\{ln\}}_{\{ij\}}(T_8)_{klm}P^m_n \\ & + b_{27}(T_{10})^{ijk}(H_{27})^{\{mn\}}_{\{ij\}}(T_8)_{klm}P^l_n \\ & + c_{27}(T_{10})^{ijm}(H_{27})^{\{kn\}}_{\{ij\}}(T_8)_{klm}P^l_n \\ & + d_{27}(T_{10})^{ijn}(H_{27})^{\{km\}}_{\{ij\}}(T_8)_{klm}P^l_n \\ & + e_{27}(T_{10})^{ikm}(H_{27})^{\{ln\}}_{\{ij\}}(T_8)_{klm}P^j_n \\ & + f_{27}(T_{10})^{ikn}(H_{27})^{\{lm\}}_{\{ij\}}(T_8)_{klm}P^j_n \\ & + a_8(T_{10})^{ijl}(H_8)^m_i(T_8)_{\{jkl\}}P^k_m \\ & + b_8(T_{10})^{ijm}(H_8)^k_i(T_8)_{\{jkl\}}P^l_m \\ & + c_8(T_{10})^{ijm}(H_8)^l_i(T_8)_{\{jkl\}}P^k_m \\ & + d_8(T_{10})^{ilm}(H_8)^j_i(T_8)_{\{jkl\}}P^k_m. \end{aligned} \tag{33}$$

As the color symmetry of Hamiltonian can help us further constrain the number of independent $SU(3)$ amplitude, as applied in octet baryon two body decays in the previous section, after considering color symmetry, the number of amplitudes corresponding to H_{27} can only be one, e_{27}, and the total amplitudes are

$$\begin{aligned}\mathcal{M}_{10\to 8+8} = {} & e_{27}(T_{10})^{ikm}(H_{27})^{\{ln\}}_{\{ij\}}(T_8)_{klm}P^j_n \\ & + a_8(T_{10})^{ijl}(H_8)^m_i(T_8)_{\{jkl\}}P^k_m \\ & + b_8(T_{10})^{ijm}(H_8)^k_i(T_8)_{\{jkl\}}P^l_m \\ & + c_8(T_{10})^{ijm}(H_8)^l_i(T_8)_{\{jkl\}}P^k_m \\ & + d_8(T_{10})^{ilm}(H_8)^j_i(T_8)_{\{jkl\}}P^k_m. \end{aligned} \tag{34}$$

By expanding the abovementioned expressions, we obtain the decay amplitudes listed in Table 3. Expressed by the IRA amplitude, we derive the following relations for amplitudes of decay channels as

$$\mathcal{M}(\Omega^-\to\Xi^0\pi^-) = \sqrt{3}\mathcal{M}(\Xi^{*0}\to\Sigma^+\pi^-). \tag{35}$$

The branching ratios of $T_{10}\to T_8P_8$ can be written as

$$\mathcal{B}(T_{10A}\to T_{8B}P_8) = \frac{\tau_A|p_{cm}|}{16\pi m_A^2}|A(T_{10A}\to T_{8B}P_8)|^2. \tag{36}$$

where τ_A is the lifetime of the initial decuplet baryon, $|p_{cm}|$ is the final-state momentum in the center-of-mass frame, and $A(T_{10A}\to T_{8B}P_8)$ is the decay amplitude. From the measured branching ratio $\mathcal{B}(\Omega^-\to\Xi^0\pi^-) = (24.3\pm 0.7)\%$, the decay amplitude is extracted as $A(\Omega^-\to\Xi^0\pi^-) = (9.66\pm 0.15)\times 10^{-4}$. Using Eq. (35), the decay amplitude for $\Xi^{*0}\to\Sigma^+\pi^-$ is derived from this result, and the corresponding branching ratio is then calculated via Eq. (36):

$$\mathcal{B}(\Xi^{*0}\to\Sigma^+\pi^-) = (8.04\pm 0.51)\times 10^{-14}. \tag{37}$$

This branching ratio is of the order of $O(10^{-14})$, consistent with theoretical expectations. The reason lies in the different dominant interactions: the Ω^- decays primarily via weak interaction and has a relatively long lifetime of 8.21×10^{-11}s, whereas Ξ^{*0} decays mainly through strong interaction, leading to a much shorter lifetime on the order of $O(10^{-23})$s. Consequently, the resulting branching ratio for the weak decay of Ξ^{*0} is significantly suppressed, as reflected in the value obtained through Eq.

Table 3. Irreducible representation amplitudes of the other hyperon two-body non-leptonic decay.

Channel	Amplitudes
$\Sigma^{*+}\to p\pi^0$	$\frac{\sin\theta(-5a_8+5b_8-5d_8+6e_{27})}{20\sqrt{6}}$
$\Sigma^{*-}\to n\pi^-$	$\frac{\sin\theta(-5a_8-5c_8-5d_8-4e_{27})}{20\sqrt{3}}$
$\Sigma^{*0}\to p\pi^-$	$\frac{\sin\theta(-5a_8+5b_8-5d_8-4e_{27})}{20\sqrt{6}}$
$\Sigma^{*0}\to n\pi^0$	$\frac{\sin\theta(-5a_8-5b_8-10c_8-5d_8+6e_{27})}{40\sqrt{3}}$
$\Omega^-\to\Xi^0\pi^-$	$\frac{\sin\theta(5a_8+4e_{27})}{20}$
$\Omega^-\to\Xi^-\pi^0$	$\frac{\sin\theta(5a_8-6e_{27})}{20\sqrt{2}}$
$\Xi^{*0}\to\Sigma^+\pi^-$	$\frac{\sin\theta(5a_8+4e_{27})}{20\sqrt{3}}$
$\Xi^{*0}\to\Sigma^0\pi^0$	$\frac{\sin\theta(5a_8-5b_8-5c_8-6e_{27})}{40\sqrt{3}}$
$\Xi^{*-}\to\Sigma^0\pi^-$	$\frac{\sin\theta(-5a_8-5b_8-5c_8-4e_{27})}{20\sqrt{6}}$
$\Xi^{*-}\to\Sigma^-\pi^0$	$\frac{\sin\theta(5a_8+5b_8+5c_8-6e_{27})}{20\sqrt{6}}$
$\Xi^{*0}\to\Lambda^0\pi^0$	$\frac{\sin\theta(15a_8-5b_8+5c_8+10d_8-18e_{27})}{120}$
$\Xi^{*-}\to\Lambda^0\pi^-$	$\frac{\sin\theta(15a_8-5b_8+5c_8+10d_8+12e_{27})}{60\sqrt{2}}$
$\Xi^{*0}\to pK^-$	$\frac{\sin\theta(b_8-d_8)}{4\sqrt{3}}$
$\Xi^{*-}\to nK^-$	$\frac{\sin\theta(-c_8-d_8)}{4\sqrt{3}}$
$\Omega^-\to\Lambda^0K^-$	$\frac{\sin\theta(-b_8+c_8+2d_8)}{4\sqrt{6}}$
$\Xi_c^+\to\Lambda_c^+\pi^0$	$\frac{\sin\theta(5a_8-6a_{27})}{20\sqrt{2}}$
$\Xi_c^0\to\Lambda_c^+\pi^-$	$\frac{\sin\theta(5a_8+4a_{27})}{20}$
$\Xi_c'^+\to\Lambda_c^+\pi^0$	$\frac{\sin\theta(-5a_8-5b_8+6b_{27})}{40}$
$\Xi_c'^0\to\Lambda_c^+\pi^-$	$\frac{\sin\theta(-5a_8-5b_8-4b_{27})}{20\sqrt{2}}$
$\Omega_c^0\to\Xi_c^0\pi^0$	$\frac{\sin\theta(5a_8-6b_{27})}{20\sqrt{2}}$
$\Omega_c^0\to\Xi_c^+\pi^-$	$\frac{\sin\theta(-5a_8-4b_{27})}{20}$

(36).

We consider the two decay channels $\Omega^- \to \Xi^0\pi^-$ and $\Omega^- \to \Xi^-\pi^0$ to extract the parameters a_8 and e_{27} by fitting to Eq. (25), using the corresponding branching ratios $\mathcal{B}(\Omega^- \to \Xi^0\pi^-) = (24.3 \pm 0.7)\%$, $\mathcal{B}(\Omega^- \to \Xi^-\pi^0) = (8.55 \pm 0.33)\%$, and the symmetric parameters $\alpha(\Omega^- \to \Xi^0\pi^-) = 0.09 \pm 0.14$, $\alpha(\Omega^- \to \Xi^-\pi^0) = 0.05 \pm 0.21$. Due to the large experimental uncertainties in the symmetric parameters α extracted from the decays $\Omega^- \to \Xi^0\pi^-$ and $\Omega^- \to \Xi^-\pi^0$, these parameters are neglected in the present analysis. For the analysis of the decay branching ratios, we define the amplitudes in Eq. (36) for these two channels as

$$\begin{aligned} \left|A(\Omega^- \to \Xi^0\pi^-)\right| &= \frac{\sin\theta(5a_8 + 4e_{27})}{20}, \\ \left|A(\Omega^- \to \Xi^-\pi^0)\right| &= \frac{\sin\theta(5a_8 - 6e_{27})}{20\sqrt{2}}. \end{aligned} \tag{38}$$

Then, the experimental data can be used to determine these amplitudes as

$$a_8 = 0.3228 \pm 0.0037, \quad e_{27} = 0.027 \pm 0.0037. \tag{39}$$

As expected from our previous discussion, the amplitude e_{27} contributes less than a_8.

With the fitted amplitude, we can make some predictions by extracting the parameter $D_8 = -b_8 + c_8 + 2d_8 = 1.8087 \pm 0.0094$ from the experimental data $\mathcal{B}(\Omega^- \to \Lambda^0 K^-) = (67.7 \pm 0.7)\%$ using Eq. (25). This leads to the IRA amplitudes for $\Xi^{*0} \to \Lambda^0\pi^0$ and $\Xi^{*-} \to \Lambda^0\pi^-$ becoming

$$\begin{aligned} \left|A(\Xi^{*0} \to \Lambda^0\pi^0)\right| &= \frac{\sin\theta(15a_8 + 5D_8 - 18e_{27})}{120}, \\ \left|A(\Xi^{*-} \to \Lambda^0\pi^-)\right| &= \frac{\sin\theta(15a_8 + 5D_8 + 12e_{27})}{60\sqrt{2}}. \end{aligned} \tag{40}$$

However, due to an unknown phase angle ϕ between D_8 and a_8, e_{27}, the exact amplitudes for these two decay channels cannot be determined. Our results provide the range of branching ratios for different values of the phase angle ϕ.

$$\begin{aligned} &4.59 \times 10^{-14} \leq \mathcal{B}(\Xi^{*0} \to \Lambda^0\pi^0) \leqslant 4.16 \times 10^{-13}, \\ &4.87 \times 10^{-14} \leq \mathcal{B}(\Xi^{*-} \to \Lambda^0\pi^-) \leqslant 8.65 \times 10^{-13}. \end{aligned} \tag{41}$$

These predictions can be tested in future high-precision experiments.

B. Charmed baryon two body decay induced by $s \to d$

Induced by the $s \to d$ Hamiltonian, charmed baryon containing the strange quark, such as $\{\Xi_c'^+, \Xi_c'^0\}$, can also decay into $\{\Xi_c^{+/0}, \Lambda_c\}$. Depending on whether the initial charmed baryon is an anti-triplet or a sextet baryon, the discussion can be further divided into two cases. The anti-triplet $T_{c\bar{3}}$ and sextet T_{c6} under $SU(3)$ flavor symmetry can be written as

$$\begin{aligned} T_{c\bar{3}} &= \begin{pmatrix} 0 & \Lambda_c^+ & \Xi_c^+ \\ -\Lambda_c^+ & 0 & \Xi_c^0 \\ -\Xi_c^+ & -\Xi_c^0 & 0 \end{pmatrix}, \\ T_{c6} &= \begin{pmatrix} \Sigma_c^{++} & \frac{\Sigma_c^+}{\sqrt{2}} & \frac{\Xi_c'^+}{\sqrt{2}} \\ \frac{\Sigma_c^+}{\sqrt{2}} & \Sigma_c^0 & \frac{\Xi_c'^0}{\sqrt{2}} \\ \frac{\Xi_c'^+}{\sqrt{2}} & \frac{\Xi_c'^0}{\sqrt{2}} & \Omega_c^0 \end{pmatrix}. \end{aligned} \tag{42}$$

Here, the $SU(3)$ flavour anti-triplet charmed baryons can also be represented as $(T_{c\bar{3}})_i = \epsilon_{ijk}(T_{c\bar{3}})^{[jk]} = (\Xi_c^0, -\Xi_c^+, \Lambda_c^+)$. Following the same method, the irreducible representation amplitudes of decay $T_{c\bar{3}}$ and T_{c6} can be constructed.

The amplitude for the two body decays of $T_{c\bar{3}}$ is given as

$$\begin{aligned} \mathcal{M}_{T_{c\bar{3}} \to T_{c\bar{3}} P_8} = {} & a_{27}(T_{c\bar{3}})_i (H_{27})^{\{il\}}_{\{jk\}} (T_{c\bar{3}})^j P_l^k \\ & + a_8 (T_{c\bar{3}})_i (H_8)^k_j (T_{c\bar{3}})^j P_k^i. \end{aligned} \tag{43}$$

To exclude the color suppressed amplitude of these processes, the TDA amplitudes are needed. The detailed discussion of TDA amplitude can be found in the appendix. A comparison with the topological diagrammatic approach (TDA) amplitudes reveals that the irreducible representation amplitudes (IRA) constructed in Eq. (43) are not subject to color suppression.

The amplitude for the two body decays of T_{c6} is given as

$$\begin{aligned} \mathcal{M}_{T_{c6} \to T_{c\bar{3}} P_8} = {} & a_{27} (T_{c6})^{\{ij\}} (H_{27})^{\{km\}}_{\{ij\}} (T_{c\bar{3}})_{[kl]} P^l_m \\ & + b_{27} (T_{c6})^{\{ik\}} (H_{27})^{\{lm\}}_{\{ij\}} (T_{c\bar{3}})_{[kl]} P^j_m \\ & + a_8 (T_{c6})^{\{ij\}} (H_8)^l_i (T_{c\bar{3}})_{[jk]} P^k_l \\ & + b_8 (T_{c6})^{\{il\}} (H_8)^j_i (T_{c\bar{3}})_{[jk]} P^k_l. \end{aligned} \tag{44}$$

After excluding the color suppressed amplitude, we obtain

$$\begin{aligned}\mathcal{M}_{T_{c6}\to T_{c\bar{3}}P_8} &= b_{27}\,(T_{c6})^{\{ik\}}\,(H_{27})^{\{lm\}}_{\{ij\}}\,(T_{c\bar{3}})_{[kl]}\,P^j_m \\ &+ a_8\,(T_{c6})^{\{ij\}}\,(H_8)^l_i\,(T_{c\bar{3}})_{[jk]}\,P^k_l \\ &+ b_8\,(T_{c6})^{\{il\}}\,(H_8)^j_i\,(T_{c\bar{3}})_{[jk]}\,P^k_l. \end{aligned} \tag{45}$$

Expanding the above equations, we will obtain the decay amplitudes given in Table 3.

For heavy-flavor conserving decays $\Xi_c^+\to\Lambda_c^+\pi$ and $\Omega_c^0\to\Xi_c^0\pi$, the contribution from transition $cs\to dc$ is also important, as $V_{cd}V_{cs}^*\sim V_{ud}V_{us}^*\sim\sin\theta$. Within the $SU(3)$ framework, the Hamiltonian H^i_j for the transition $cs\to dc$ can be decomposed as

$$H^i_j=\left(H^i_j-\frac{1}{3}\delta^i_jH^k_k\right)+\frac{1}{3}\delta^i_jH^k_k=(H_8)^i_j+\frac{1}{3}\delta^i_jH_1. \tag{46}$$

By decomposing this Hamiltonian into its irreducible representations, one obtains an octet and a singlet component. As the contribution from the singlet is negligibly small, it is not taken into account. For the octet Hamiltonian of the $cs\to dc$ transition, the only non-zero component is $(H_8)^2_{\bar{3}}=\sin\theta$. This corresponds to the non-zero component $(H_8)^2_{\bar{3}}=1/4\sin\theta$ in the octet Hamiltonian of the $s\to du\bar{u}$ transition, differing only by a coefficient. Therefore, the irreducible representation amplitude for $cs\to dc$ can be absorbed into our existing results and does not affect our final calculations.

V. CONCLUSION

In this work, we investigated the baryon two decay processes induced by $s\to d\bar{u}u$. The hyperon two body decays with $\Delta S=1$ are primarily driven by this Hamiltonian, which is the central focus of our study. Under the $SU(3)$ flavor symmetry, the baryon two body decays can be easily expressed by several IRA amplitudes. For constructing the $SU(3)$ irreducible amplitude, the Hamiltonian corresponding to $s\to d\bar{u}u$ must be decomposed as $3\otimes3\otimes\bar{3}\otimes\bar{3}=27\oplus10\oplus\overline{10}\oplus8\oplus8\oplus8\oplus8\oplus1\oplus1$. Fortunately, under the symmetric and antisymmetric transformations, the expression of each irreducible representation can be derived using Eq. (14). After including the correlation of symmetry of quark field and anti-quark field, the decuplet Hamiltonian will automatically disappear and only octet and 27-plet can contribute.

Using the decomposed Hamiltonian, we can finally construct the IRA amplitude, and by considering the color information in the baryon state and Hamiltonian, the number of independent amplitudes can be reduced to six. As we expected, the flavor symmetry is not a good symmetry in hyperon decays. Therefore, we systemically introduced a symmetry breaking effect induced by the difference of quark mass. With the symmetry breaking effect, we can perform a global analysis of the hyperon two decay processes. Our analysis shows that the $\mathrm{Br}(\Sigma^+\to p\pi^0)$ and $\alpha(\Sigma^+\to p\pi^0)$ deviate from our predictions by more than 1σ. This puzzle cannot be explained by the $SU(3)$ symmetry breaking effect, suggesting potential contributions from other mechanisms. Besides, we find that the symmetry breaking effect in amplitude corresponding to H_{27} is at lest 75%, and our results indicate these processes may contain a large symmetry breaking effect of approximately 1000%. We strongly recommend that future experimental efforts aim to reduce measurement uncertainties, especially for the processes $\Lambda^0\to p\pi^-$ and $\Lambda^0\to n\pi^0$, which have larger experimental errors compared to other data and play an important role in determining the parameter $\mathbf{c}^2_{\mathbf{27}}$. Then, the extent of $SU(3)$ symmetry breaking can be determined with higher precision. With the help of current experiment data, we can determine part of the amplitude, and the branching ratios of $\Xi^{*0}\to\Lambda^0\pi^0$ and $\Xi^{*-}\to\Lambda^0\pi^-$ can be estimated. However, due to the lack of experimental data, the phase of amplitude cannot be determined. Therefore, we can only provide the possible range of branching ratio in Eq. (41) by varying its phase from 0 to π. In the last part of this paper, we also analyzed the two body decays of charmed baryons induced by $s\to d$. However, due to a lack of experimental data, we can only present the expressions for the amplitude.

ACKNOWLEDGEMENTS

We thank Dr. Xiao hui Hu in CUMT and Dr. Yuji Shi in ECUST for their useful discussions.

APPENDIX A

In Section V, to simplify the IRA further, we also investigated the TDA of the two-body decays of charmed baryons in the anti-triplet $T_{c\bar{3}}$ and charmed baryons in the anti-sextet $T_{c\bar{6}}$, caused by light quarks $s\to u\bar{u}d$. For the $s\to u\bar{u}d$ decays, the non-zero components of the effective Hamiltonian are

$$H^{12}_{13}=\sin\theta. \tag{A1}$$

The amplitudes of processes $T_{c\bar{3}}\to T_{c\bar{3}}P_8$ and $T_{c\bar{6}}\to T_{c\bar{3}}P_8$ in topological diagrammatic approach (TDA) can be written as

$$\begin{aligned}\mathcal{M}_{T_{c\bar{3}}\to T_{c\bar{3}}P_8} &= a_1(T_{c\bar{3}})^{[jk]}H^{ml}_{ij}(T_{c\bar{3}})_{[kl]}P^i_m \\ &+ a_2(T_{c\bar{3}})^{[jk]}H^{lm}_{ij}(T_{c\bar{3}})_{[kl]}P^i_m \\ &+ a_3(T_{c\bar{3}})^{[ij]}H^{km}_{ij}(T_{c\bar{3}})_{[kl]}P^l_m \\ &+ a_4(T_{c\bar{3}})^{[jm]}H^{kl}_{ij}(T_{c\bar{3}})_{[kl]}P^i_m \\ &+ a_5(T_{c\bar{3}})^{[jk]}H^{im}_{ij}(T_{c\bar{3}})_{[kl]}P^l_m \\ &+ a_6(T_{c\bar{3}})^{[jm]}H^{ik}_{ij}(T_{c\bar{3}})_{[kl]}P^l_m. \end{aligned} \tag{A2}$$

$$\begin{aligned}\mathcal{M}_{T_{c\bar{6}}\to T_{c\bar{3}}P_8} = & b_1(T_{c\bar{6}})^{\{jk\}}H^{ml}_{ij}(T_{c\bar{3}})_{[kl]}P^i_m \\ & + b_2(T_{c\bar{6}})^{\{jk\}}H^{lm}_{ij}(T_{c\bar{3}})_{[kl]}P^i_m \\ & + b_3(T_{c\bar{6}})^{\{ij\}}H^{km}_{ij}(T_{c\bar{3}})_{[kl]}P^l_m \\ & + b_4(T_{c\bar{6}})^{\{jm\}}H^{kl}_{ij}(T_{c\bar{3}})_{[kl]}P^i_m \\ & + b_5(T_{c\bar{6}})^{\{jk\}}H^{im}_{ij}(T_{c\bar{3}})_{[kl]}P^l_m \\ & + b_6(T_{c\bar{6}})^{\{jm\}}H^{ik}_{ij}(T_{c\bar{3}})_{[kl]}P^l_m. \end{aligned} \tag{A3}$$

The relevant topological diagrams for $T_{c\bar{3}} \to T_{c\bar{3}}P_8$ and $T_{c\bar{6}} \to T_{c\bar{3}}P_8$ nonleptonic weak decays are displayed in Fig. A1. The topological diagrams in Fig. A1 can be divided into three categories: the tree diagrams in Fig. A1 (a, b), the W-exchange diagrams in Fig. A1 (c, d), and the penguin diagrams in Fig. A1 (e, f).

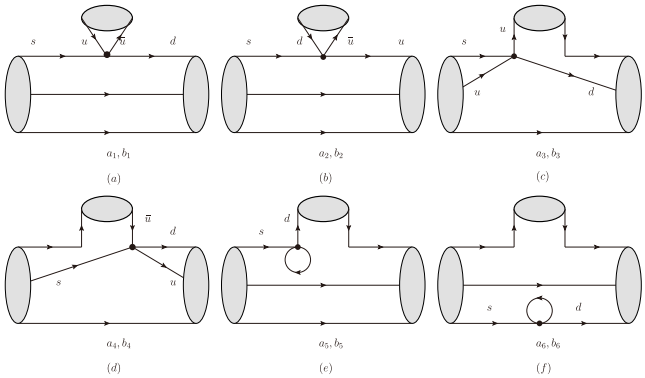

Fig. A1. Topological diagrams for $T_{c\bar{3}} \to T_{c\bar{3}}P_8$ and $T_{c\bar{6}} \to T_{c\bar{3}}P_8$ nonleptonic decays.

References

[1] M. Ablikim *et al.* (BESIII), Phys. Rev. D **97**(3), 032013 (2018), arXiv: 1709.10236[hep-ex]
[2] R. Aaij *et al.* (LHCb), Phys. Rev. Lett. **120**(22), 221803 (2018), arXiv: 1712.08606[hep-ex]
[3] R. Aaij *et al.* (LHCb), Sci. Bull. **66**, 1278 (2021), arXiv: 2012.10380[hep-ex]
[4] M. Ablikim *et al.* (BESIII), Phys. Rev. Lett. **129**(13), 131801 (2022), arXiv: 2204.11058[hep-ex]
[5] M. Ablikim *et al.* (BESIII), Phys. Rev. Lett. **129**(21), 212002 (2022), arXiv: 2206.10791[hep-ex]
[6] M. Ablikim *et al.* (BESIII), Phys. Rev. Lett. **130**(21), 211901 (2023), arXiv: 2302.13568[hep-ex]
[7] M. Ablikim *et al.* (BESIII), Phys. Lett. B **852**, 138614 (2024), arXiv: 2312.17063[hep-ex]
[8] M. Ablikim *et al.* (BESIII), Phys. Rev. D **108**(9), L091101 (2023), arXiv: 2309.06368[hep-ex]
[9] X. G. He and J. P. Ma, Phys. Lett. B **839**, 137834 (2023), arXiv: 2212.08243[hep-ph]
[10] M. Gockeler *et al.* (QCDSF), Phys. Lett. B **545**, 112 (2002), arXiv: hep-lat/0208017[hep-lat]
[11] Z. P. Xing, Y. J. Shi, J. Sun *et al.*, arXiv: 2312.17568[hep-ph]
[12] J. Fu, H. B. Li, J. P. Wang *et al.*, Phys. Rev. D **108**(9), 9 (2023), arXiv: 2307.04364[hep-ex]
[13] E. N. Dubovik, V. S. Zamiralov, S. Lepshokov *et al.*, Phys. Atom. Nucl. **71**, 136 (2008)
[14] X. H. Hu and Z. X. Zhao, Chin. Phys. C **43**(9), 093104 (2019), arXiv: 1811.01478[hep-ph]
[15] P. Zenczykowski, Acta Phys. Polon. B **51**, 2111 (2020), arXiv: 2009.12552[hep-ph]
[16] J. P. Wang and F. S. Yu, Phys. Lett. B **849**, 138460 (2024), arXiv: 2208.01589[hep-ph]
[17] P. Zenczykowski, Phys. Rev. D **62**, 014030 (2000), arXiv: hep-ph/9911267[hep-ph]
[18] R. X. Shi, S. Y. Li, J. X. Lu *et al.*, Sci. Bull. **67**, 2298 (2022), arXiv: 2206.11773[hep-ph]
[19] R. X. Shi and L. S. Geng, Sci. Bull. **68**, 779 (2023), arXiv: 2303.18002[hep-ph]
[20] C. Han and J. Zhang, Phys. Rev. D **109**(1), 014034 (2024), arXiv: 2311.02669[hep-ph]
[21] R. X. Shi, Z. Jia, L. S. Geng *et al.*, Chin. Phys. Lett. **42**(3), 032401 (2025), arXiv: 2502.15473[hep-ph]
[22] R. M. Wang, M. Z. Yang, H. B. Li *et al.*, Phys. Rev. D **100**(7), 076008 (2019), arXiv: 1906.08413[hep-ph]
[23] Y. G. Xu, X. D. Cheng, J. L. Zhang *et al.*, J. Phys. G **47**(8), 085005 (2020), arXiv: 2001.06907[hep-ph]
[24] P. Y. Niu, J. M. Richard, Q. Wang *et al.*, Chin. Phys. C **45**(1), 013101 (2021), arXiv: 2007.09621[hep-ph]
[25] G. S. Bali, V. M. Braun, S. Bürger *et al.*, arXiv: 2411.19091 [hep-lat]
[26] M. H. Chu *et al.* (Lattice Parton), Phys. Rev. D **111**(3), 034510 (2025), arXiv: 2411.12554[hep-lat]
[27] D. Chang, arXiv: 0011163[hep-ph]
[28] H. B. Li, Front. Phys. (Beijing) **12**(5), 121301 (2017) [Erratum: Front. Phys. (Beijing) **14**(6), 64001 (2019)], arXiv: 1612.01775[hep-ex]
[29] X. G. He, J. Tandean, and G. Valencia, Phys. Rev. D **108**(5), 055012 (2023), arXiv: 2304.02559[hep-ph]
[30] P. Zenczykowski, Phys. Rev. D **73**, 076005 (2006), arXiv: hep-ph/0512122[hep-ph]
[31] G. Buchalla, A. J. Buras, and M. E. Lautenbacher, Rev. Mod. Phys. **68**, 1125 (1996), arXiv: hep-ph/9512380[hep-ph]
[32] Y. J. Shi, Y. Xing, and Z. X. Zhao, Eur. Phys. J. C **81**(2), 156 (2021), arXiv: 2012.12613[hep-ph]
[33] J. G. Korner, Nucl. Phys. B **25**, 282 (1971)
[34] J. C. Pati and C. H. Woo, Phys. Rev. D **3**, 2920 (1971)
[35] X. G. He and W. Wang, Chin. Phys. C **42**(10), 103108 (2018), arXiv: 1803.04227[hep-ph]
[36] X. G. He, Y. J. Shi, and W. Wang, Eur. Phys. J. C **80**(5), 359 (2020), arXiv: 1811.03480[hep-ph]
[37] P..Lepage and C. Gohlke, gplepage/lsqfit: lsqfit version 11.7 (v11.7), Zenodo, http://dx.doi.org/10.5281/zenodo.4037174